[Chem. Pharm. Bull. 27(11)2710—2717(1979)]

UDC 546.711.04.08 : 612.014.1 : 541.133.1

Concentration of Manganese by Reverse Permeation across a Cellulose Membrane

Fujio Kametani, Shuji Kitagawa,[1a] and Keitaro Nishiyama[1b]

Faculty of Pharmaceutical Sciences, University of Tokushima[1a] *and School of Medicine, University of Tokushima*[1b]

(Received April 16, 1979)

The reverse permeation of Mn^{2+} across a cellulose membrane in $CaCl_2$–$MnCl_2$–H_2O and NaCl–$MnCl_2$–H_2O systems was studied. The reverse permeation of an ion is described by equation (1) which consists of two terms, *i.e.*, the electric potential gradient and concentration gradient terms. When the flux of an ion due to the electric potential gradient is large and opposite in direction to that due to the concentration gradient, reverse permeation can occur, *i.e.*, concentration of the solute into the compartment with higher concentration. In both systems, Mn^{2+} (even at low concentrations) was concentrated in one compartment of the permeation cell by reverse permeation. The concentration of Mn^{2+} was more effective in the presence of Ca^{2+} than Na^+. The experimental values were in good agreement with Güntelberg's approximations.

Keywords——cellulose membrane; concentration effect; diffusion potential; manganese; mixed electrolytes; permeability; permeation flux; reverse permeation

Introduction

Migration of an ion against its concentration gradient in a mixed electrolytes solution, reverse diffusion, can occur as a result of the diffusion potentials of coexisting ions.[2] Permeation of an ion across a membrane from a low concentration solution to a high concentration solution, reverse permeation, can also occur.[3] In these papers, the importance of the membrane potential in ion transport is indicated, and it is suggested that reverse permeation may be involved in the transport of ions in biological systems. Even in a simple model system, however, the conditions under which reverse permeation can be observed have not been determined, and the degree of concentration that can occur is also unknown.

Manganese can be concentrated from the soil into plants. It is also retained in the human body at a concentration three or four times that in food. The availability of manganese to plants is also affected by soil characteristics, other cations and total salts.[4] Heavy fertilization of soil with chlorides may increase manganese availability to plants.

The concentration of Mn^{2+} was studied in this paper in $CaCl_2$–$MnCl_2$–H_2O and NaCl–$MnCl_2$–H_2O model systems using a cellulose membrane. In the $CaCl_2$–$MnCl_2$–H_2O system, the initial concentrations of Ca^{2+} in both compartments of the permeation cell and that of Mn^{2+} in the compartment of lower concentration were fixed. Changes in the concentration of Mn^{2+} in the compartment of higher concentration were measured. Similar experiments were carried out on the NaCl–$MnCl_2$–H_2O system with various coexisting cations. Moreover, the changes of permeation flux were measured in these systems. The significance of the results is discussed.

---

[1] Location: *a) Shomachi-1, Tokushima, 770, Japan*; *b) Kuramotocho-3, Tokushima, 770, Japan.*

[2] M. Nakagaki and S. Kitagawa, *Bull. Chem. Soc. Japan*, **49**, 1748 (1976).

[3] M. Nakagaki and S. Kitagawa, *Yakugaku Zasshi*, **98**, 840 (1978).

[4] Committee on Biologic Effects of Atmospheric Pollutants, "Manganese," National Academy of Sciences, Washington, D.C., 1973, p. 51.

Theoretical

The membrane permeation flux of any ion in mg-ion$\cdot$cm$^{-2}\cdot$s^{-1}, $[Ji]$, is given by the following equation, which consists of two terms involving the concentration gradient and electrical gradient.[2,3,5]

$$[J_\mathrm{i}] = -fD_\mathrm{i}(\partial[i]/\partial x) - (f[i]B_\mathrm{i}Z_\mathrm{i}F_\mathrm{A}/N_\mathrm{A})(\partial E/\partial x) \qquad (1)$$

Here, $[i]$ is the concentration in mg-ion$\cdot$l^{-1} of the ion, E is the electrical potential and x is the coordinate taken in the direction of the flux. Di, Bi and Zi are the diffusion coefficient, mobility and valence of the ion i, respectively. Moreover, f is the membrane constant which represents the porosity of the membrane; F_A and N_A are the Faraday and Avogadro constants, respectively.

The membrane permeability coefficient of the ion is defined by

$$[J_\mathrm{i}] = -P_\mathrm{i}(\partial[i]/\partial x) \qquad (2)$$

In the steady state, the following equation can be derived from equation (1) according to Wendt.[5]

$$P_\mathrm{i} = -fkTB_\mathrm{i}\left\{1-\frac{Z_\mathrm{i}[i]\sum_\mathrm{n} Z_\mathrm{n}B_\mathrm{n}h_\mathrm{n}\partial[n]/\partial x}{(h_\mathrm{i}\sum_\mathrm{n} Z_\mathrm{n}^2B_\mathrm{n}[n])(\partial[i]/\partial x)}\right\} \qquad (3)$$

Here, $\sum_\mathrm{n}$ means a sum over all ions, while hn is the coefficient with γi as the activity coefficient for the ion i.

$$h_\mathrm{i} = 1 + \partial \ln \gamma_\mathrm{i}/\partial \ln [i] \qquad (4)$$

If the second term in brackets in equation (3) is larger than unity, Pi is negative and reverse permeation of the ion can be expected. In the $CaCl_2$–$MnCl_2$–H_2O and NaCl–$MnCl_2$–H_2O systems in this study, reverse permeation of Mn^{2+} should be observed under the following condition.

$$G(1/2) < -F(1/2)\cdot\frac{\{(Z_1/Z_2)(B_1/B_3)+(|Z_3|/Z_2)\}(h_2/h_3)}{1-(B_1/B_3)(h_1/h_3)} - \frac{1+(|Z_3|/Z_2)(h_2/h_3)}{1-(B_1/B_3)(h_1/h_3)} \qquad (5)$$

Here, Cl^-, Mn^{2+} and Ca^{2+} or Na^+ are represented by the subscripts 3,2 and 1. $F(i/j)$ is the ratio of concentrations in mg-equiv$\cdot$l^{-1}, and $G(i/j)$ is the ratio of concentration gradients. They are defined by the following equations

$$F(i/j) = |Z_\mathrm{i}/Z_\mathrm{j}|\cdot([i]/[j]) \qquad (6)$$

$$G(i/j) = |Z_\mathrm{i}/Z_\mathrm{j}|\cdot(\partial[i]/\partial x)/(\partial[j]/\partial x) \qquad (7)$$

If the volumes of the compartments on both sides of the permeation cell are nearly equal, the right-hand term in equation (5) is constant, because $F(i/j)$ is independent of time in this case. Therefore, the reverse permeation of an ion could be determined from the concentration gradient ratio, as shown in Fig. 1. If Mn^{2+} migrates along its concentration gradient, it would move from compartment I to compartment II, which is indicated by the first term of equation (1). However, a diffusion potential exists between the coexisting ions, Ca^{2+} and Cl^-, which is positive in compartment I and negative in compartment II, because the mobility of Cl^- is larger than that of Ca^{2+}. Due to this gradient of electrical potentials, Mn^{2+} migrates from compartment I to compartment II, as indicated by the second term of equation (1). When the flow due to the electrical gradient is larger than that due to the concentration gradient, Mn^{2+} migrates against the concentration gradient.

---

[5] R.P. Wendt, *J. Phys. Chem.*, **69**, 1227 (1965).

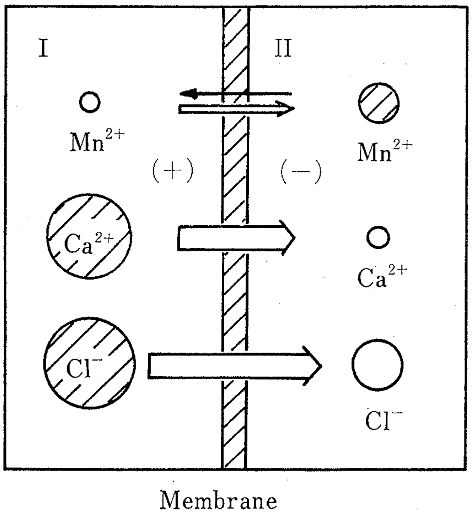

$$\begin{array}{ccc} [\mathrm{Mn}^{2+}]_{\mathrm{I}}^{0} & < & [\mathrm{Mn}^{2+}]_{\mathrm{II}}^{0} \\ \vee & & \wedge \\ [\mathrm{Mn}^{2+}]_{\mathrm{I}}^{t} & \ll & [\mathrm{Mn}^{2+}]_{\mathrm{II}}^{t} \end{array}$$

Fig. 1. Schematic Mechanism of Reverse Permeation of Mn^{2+} in the $CaCl_2$–$MnCl_2$–H_2O System

Each circle is in proportion to the ion concentration.
The width of each arrow indicates the relative flux, and its length indicates the mobility of the ion.

Experimental

Materials——Visking cellulose tubing was purchased for use as a membrane. The thickness of the membrane was 35 μ. All chemicals were of guaranteed reagent grade. Distilled and deionized water was used.

Permeation——Some constants of the permeation glass cells are shown in Table I. Each compartment was stirred magnetically at about 900 rpm in a thermostat at 25±0.1°. The concentration of Mn^{2+} was measured with an atomic absorption spectrometer (Japan Jarrell Ash Co., type AA-8200) at 279.5 nm. Background was corrected for with a D_2 lamp simultaneously. Differences in the concentration of Mn^{2+} in four experiments were within 4%. The total concentration of Ca^{2+} and Mn^{2+} in a solution was determined by titration with disodium-EDTA standard solution using Eriochrom Black T as an indicator. Cl^- was titrated with silver nitrate standard solution using fluorescein as an indicator.

Table I. Permeation Cell Constants

Cell No.	V_{I}[a] (cm^3)	V_{II}[a] (cm^3)	A[b] (cm^2)
1	13.59	13.54	1.156
2	13.80	14.18	1.179
3	13.46	13.67	1.178
4	12.97	12.87	1.138

a) Volumes of compartments I and II at 20°.
b) Area of the membrane.

Results and Discussion

Reverse Permeation of Mn^{2+} in the $CaCl_2$-$MnCl_2$-H_2O System

The initial concentrations of Ca^{2+} were 200 meq·l^{-1} in compartment I, and 0 meq·l^{-1} in compartment II. Those of Mn^{2+} in both compartments were equal, 1, 10 or 100 meq·l^{-1} as shown in Figs. 2, 3 and 4, respectively. The values of F(Ca/Mn) were calculated using the following equation,

$$F(i/j) = |Z_i/Z_j| \cdot \frac{([i]_{\mathrm{I}}^{0}+[i]_{\mathrm{II}}^{0})+([i]_{\mathrm{I}}^{t}+[i]_{\mathrm{II}}^{t})}{([j]_{\mathrm{I}}^{0}+[j]_{\mathrm{II}}^{0})+([j]_{\mathrm{I}}^{t}+[j]_{\mathrm{II}}^{t})} \qquad (8)$$

where, $[i]_{\mathrm{I}}^{0}$, $[j]_{\mathrm{I}}^{0}$, $[i]_{\mathrm{II}}^{0}$ and $[j]_{\mathrm{II}}^{0}$ are the initial concentrations of each ion in the indicated compartment, and $[i]_{\mathrm{I}}^{t}$, $[j]_{\mathrm{I}}^{t}$, $[i]_{\mathrm{II}}^{t}$ and $[j]_{\mathrm{II}}^{t}$ are the concentrations after time t.

The difference between the concentrations of Mn^{2+} in the two compartments increases with time and reaches a maximum after about 10 hours. Until this time, Mn^{2+} migrates against its concentration gradient. After the maximum, Mn^{2+} migrates with the concentration gradient. In the initial stage of permeation, the diffusion potential is marked because the concentration gradients of coexisting ions are relatively large. Therefore, the flow due to the diffusion potential is greater than that due to the concentration gradient, and reverse permeation is observed. As permeation proceeds, however, the diffusion potential gradient decreases and the concentration gradient increases. Eventually the two flows become equal to each other. Subsequently, the permeation follows the concentration gradient.[3] Ca^{2+} and Cl^- permeate with their concentration gradients, and approach their equilibrium concentrations with time.

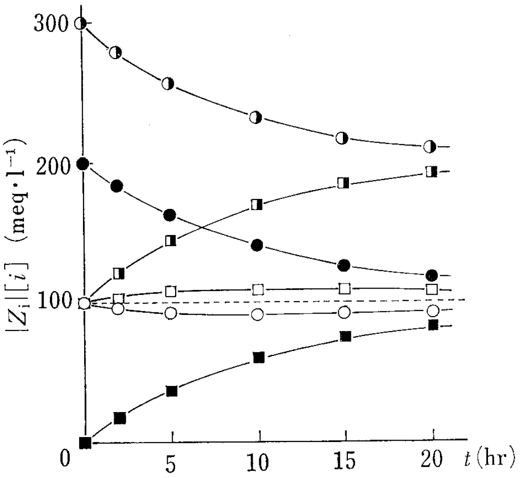

Fig. 2. Concentration Changes of Mn^{2+}, Ca^{2+} and Cl^-

Compartment I: Mn^{2+}, ○; Ca^{2+}, ●; Cl^-, ◑.
Compartment II: Mn^{2+}, □; Ca^{2+}, ■; Cl^-, ◧.
F(Ca/Mn)=1.

To compare the degree of reverse permeation under various conditions, a mean value of equivalent ion concentration can be calculated with equation (9). In this study, the compartment with higher concentration of Mn^{2+} is designated as II, and mean values of ion concentration changes can be calculated with equation (10),

$$\overline{|Z_i|[i]} = \frac{|Z_i|}{2(V_{\mathrm{I}}+V_{\mathrm{II}})}\{V_{\mathrm{I}}([i]_{\mathrm{I}}^{0}+[i]_{\mathrm{I}}^{t})+V_{\mathrm{II}}([i]_{\mathrm{II}}^{0}+[i]_{\mathrm{II}}^{t})\} \qquad (9)$$

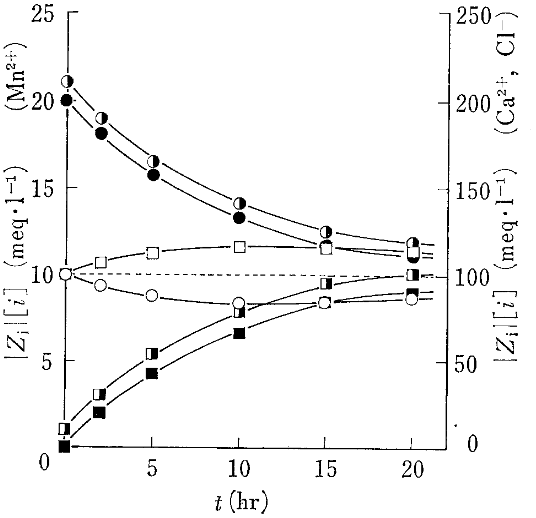

Fig. 3. Concentration Changes of Mn^{2+}, Ca^{2+} and Cl^-

Symbols are the same as in Fig. 2.
F(Ca/Mn)=10.

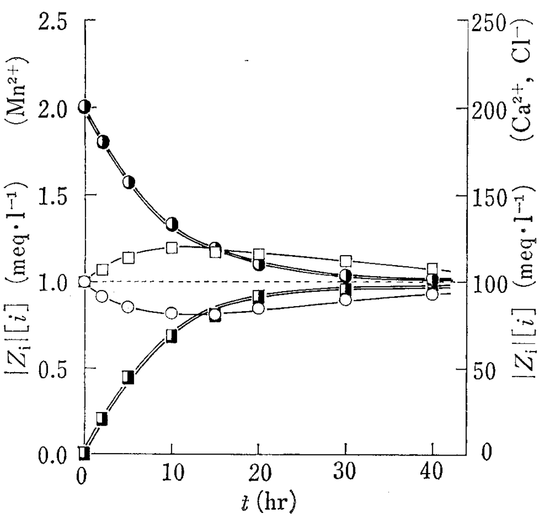

Fig. 4. Concentration Changes of Mn^{2+}, Ca^{2+} and Cl^-

Symbols are the same as in Fig. 2.
F(Ca/Mn)=100.

$$\overline{\varDelta|Z_{\mathrm{i}}|[i]} = \frac{|Z_{\mathrm{i}}|}{V_{\mathrm{I}}+V_{\mathrm{II}}}\{V_{\mathrm{I}}([i]_{\mathrm{I}}^{t}-[i]_{\mathrm{I}}^{0})+V_{\mathrm{II}}([i]_{\mathrm{II}}^{0}-[i]_{\mathrm{II}}^{t})\} \tag{10}$$

where V_{I} and V_{II} are the volumes of compartments I and II. To compare the results at various ion concentration ratios, the concentration efficiency can be calculated with equation (11). Since the numerator in the equation (11) is negative when reverse permeation is observed, equation (11) is made negative to obtain a positive value of concentration efficiency. The calculated values are shown in Fig. 5. As the concentration

$$R = -\frac{\overline{\varDelta|Z_{\mathrm{i}}|[i]}}{|Z_{\mathrm{i}}|[i]}\times 100 = -\frac{\overline{\varDelta[i]}}{[i]}\times 100\ (\%) \tag{11}$$

ratio of Ca^{2+} to Mn^{2+}, F(Ca/Mn), increases, the reverse permeation (concentration of Mn^{2+} in compartment II) shows a faster initial velocity and a larger maximum value.

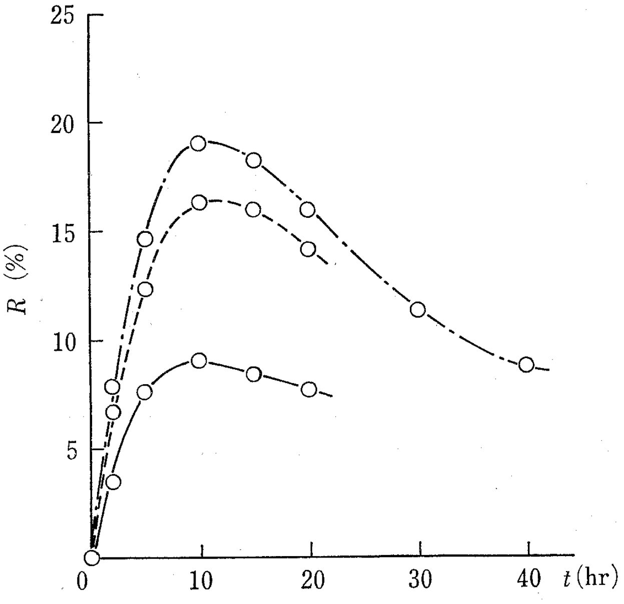

Fig. 5. Concentration Efficiency of Mn^{2+}

F(Ca/Mn): 1, (——); 10, (----); 100, (—·—).

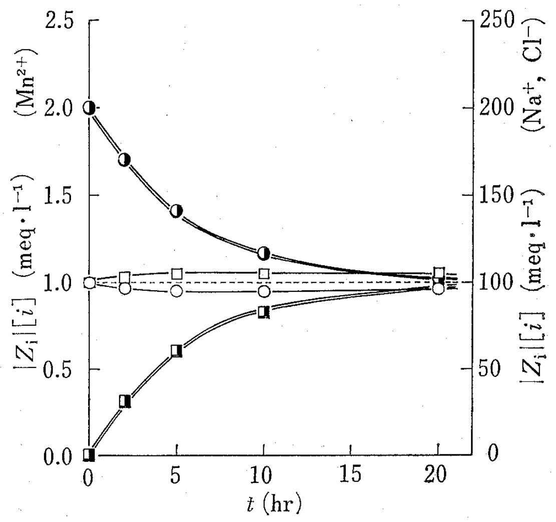

Fig. 6. Concentration Changes of Mn^{2+}, Na^+ and Cl^-

Compartment I: Mn^{2+}, ○; Na^+, ●; Cl^-, ◑.
Compartment II: Mn^{2+}, □; Na^+, ■; Cl^-, ◨.
F(Na/Mn)=100.

Reverse Permeation of Mn^{2+} in the $NaCl$-$MnCl_2$-H_2O System

In this system the initial concentration of Na^+ was 200 meq·l^{-1} in compartment I, and 0 meq-l·^{1} in compartment II; those of Mn^{2+} in both compartments were equal. The ratio of Na^+ to Mn^{2+}, F(Na/Mn), was 100. As shown in Fig. 6, the difference between the concen-

Table II. Values of Limiting Equivalent Conductivities, λ_{i}^{0} and Mobilities, B_{i} at 25°[a]

Ions	λ_{i}^{0} ($\Omega^{-1}\cdot$cm$^2\cdot$g-eq^{-1})	$B_{\mathrm{i}}\times 10^9$ (cm·sec$^{-1}\cdot$dyn^{-1})
Mn^{2+}	53.5	0.173
Ca^{2+}	59.50	0.192
Na^+	50.10	0.324
Cl^-	76.35	0.494

[a] G.C. Benson, A.R. Gordon, *J. Chem. Phys.*, **13**, 470, 473 (1945), cf. Landolt-Börnstein, "Zahlenwerte und Funktionen aus Physik, Chemie, Astronomie, Geophysik und Technik," Vol. 2 Part 7, Springer-Verlag, Berlin, Göttingen, Heidelberg, 1960, p. 257.

trations of Mn^{2+} in the two compartments increased with time and reached a maximum value after 10 hours. The magnitude of the concentration difference in this system is smaller than that in the $CaCl_2$ system. This is due to the difference of driving forces, *i.e.*, the diffusion potentials in the two systems. Since the difference of mobilities between Ca^{2+} and Cl^- is larger than that between Na^+ and Cl^-, the diffusion potential in the $CaCl_2$ system is larger than that in the NaCl system. The values of equivalent conductivities at infinite dilution λ_i^0 and mobilities Bi at 25° are listed in Table II.

Measurement and Prediction of the Maximum Concentration Value for Mn^{2+} by Reverse Permeation

The maximum concentration values for Mn^{2+} in compartment II were determined for various concentrations of Mn^{2+} in compartment I. The initial concentrations of Ca^{2+} or Na^+ in compartments I and II were 200 and 0 $meq \cdot l^{-1}$, respectively. The ratio of concentration gradients was calculated with the following equation instead of equation (7).

$$G(i/j) = |Z_i/Z_j| \cdot ([i]_{I}-[i]_{II})/([j]_{I}-[j]_{II}) \qquad (12)$$

As shown in Table III, the concentration of Mn^{2+} is affected more by Ca^{2+} than by Na^+. This is due to the difference of diffusion potentials between these systems. Table III also shows that a low concentration of Mn^{2+} compared to the concentrations of coexisting ions produces a greater Mn^{2+} concentration effect.

To study the agreement of the experimental values with the theoretical ones, the initial concentration of Mn^{2+} in compartment II, which contained no other cations, was varied. The initial concentrations of Mn^{2+} and Ca^{2+} or Na^+ in compartment I were 1 and 200 $meq \cdot l^{-1}$, respectively. The mean values of equivalent concentration changes are shown in Figs. 7 and 8. The mean values of concentration changes are shown in Figs. 9, 10 and 11. In the $CaCl_2$ system, the concentration of Mn^{2+} in compartment II reached a maximum value in a shorter time. When the initial concentration of Mn^{2+} was more than 6 $meq \cdot l^{-1}$, no concentration effect could be observed. It is suggested that the concentration factor is six. Since the concentrations of coexisting ions had already changed after one hour, this experimental result, 6, is consistent with the theoretical value, 6.6, calculated with the activity coefficients estimated by Güntelberg's approximation.6) In the NaCl system, no concentration effect

TABLE III. Calculated Limiting Concentration Values of Mn^{2+}

$Z_{Mn}[Mn]_I^0$ ($meq \cdot l^{-1}$)	$Z_{Mn}[Mn]_{II}^0$ ($meq \cdot l^{-1}$)		$[Mn]_{II}^0/[Mn]_I^0$	
	$f_i=1$a)	Güntelbergb)	$f_i=1$a)	Güntelbergb)
System: $CaCl_2$–$MnCl_2$–H_2O				
100	156	167	1.6	1.7
10	31	37	3.1	3.7
1.0	4.8	6.6	4.8	6.6
0.10	0.53	0.79	5.3	7.9
↓			↓	↓
0.00			5.4	8.1
System: NaCl–$MnCl_2$–H_2O				
100	131	133	1.3	1.3
10	20	20	2.0	2.0
1.0	2.3	2.2	2.3	2.2
0.10	0.24	0.23	2.4	2.3
↓			↓	↓
0.00			2.4	2.3

a) Theoretical Values for Activity Coefficient, $f_i=1$.
b) Theoretical Values for Activity Coefficients estimated by Güntelberg's Approximation.6)

---

6) E. Güntelberg, *Z. Phys. Chem.*, 123, 199 (1926).

could be observed at Mn^{2+} concentrations in compartment II higher than 2 meq·l⁻¹. This is also consistent with the theoretical value calculated with the activity coefficients estimated by Güntelberg's approximation. The results indicate that Ca^{2+} has a greater effect than Na^+ on the concentration of Mn^{2+}.

Flux Change with Time

The flux decreases with time in an ordinary transport system. In a mixed electrolytes solution, however, the flux change of the ions is expected to be complicated because there

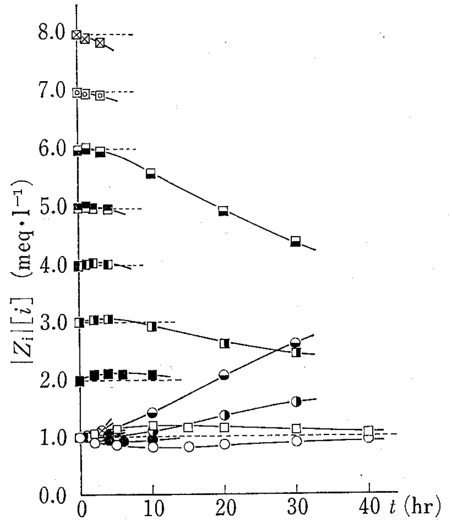

Fig. 7. Concentration of Mn^{2+} in the $CaCl_2$–$MnCl_2$–H_2O System

Circles and squares indicate the experimental points for $Z_{Mn}[Mn]^t_I$ and $Z_{Mn}[Mn]^t_{II}$, respectively. $Z_{Mn}[Mn]^0_I$: 1 meq·l⁻¹. $Z_{Mn}[Mn]^0_{II}$: 1.0, (○,□); 2.0, (●,■); 3.0, (◑,◨); 4.0, (◐,◧); 5.0, (◓,⬒); 6.0, (◒,⬓); 7.0, (◎,▣); 8.0, (⊗,⊠) meq·l⁻¹.

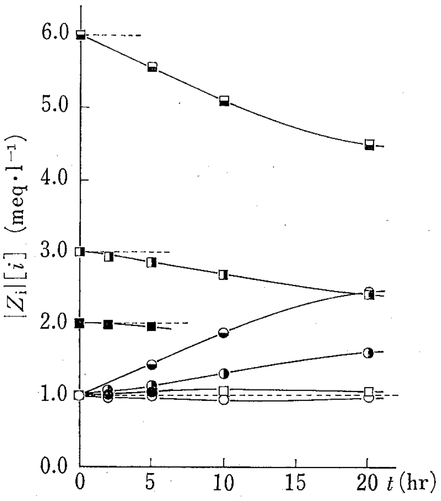

Fig. 8. Concentration of Mn^{2+} in the $NaCl$–$MnCl_2$–H_2O System

Symbols are the same as in Fig. 7.

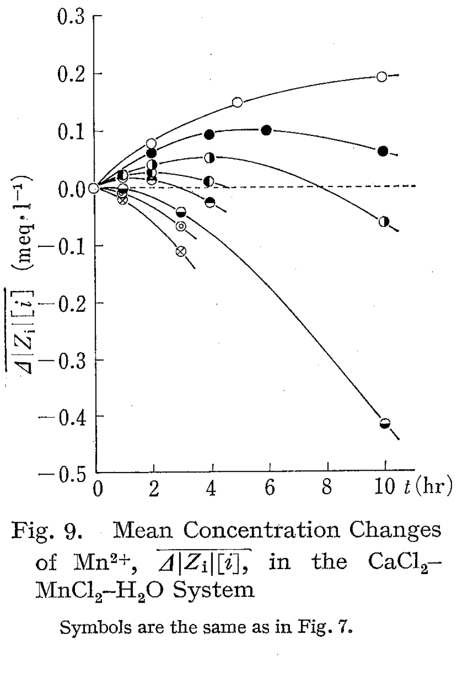

Fig. 9. Mean Concentration Changes of Mn^{2+}, $\overline{\Delta|Z_i|[i]}$, in the $CaCl_2$–$MnCl_2$–H_2O System

Symbols are the same as in Fig. 7.

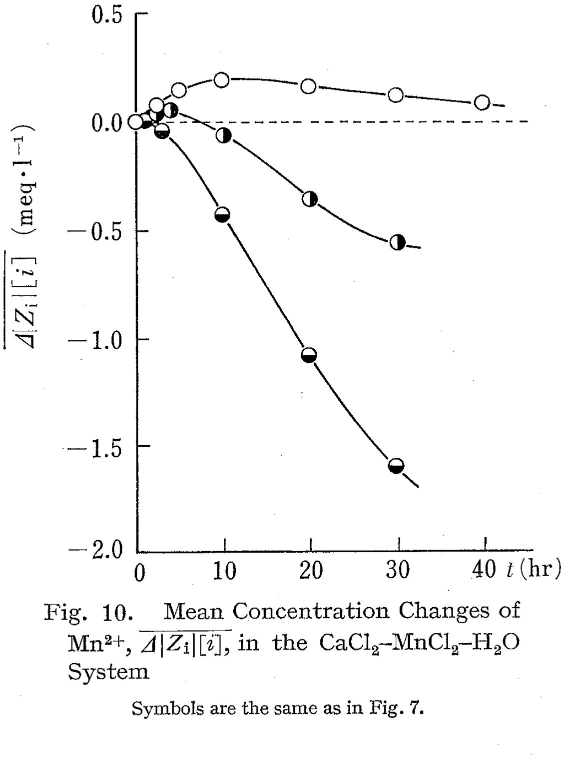

Fig. 10. Mean Concentration Changes of Mn^{2+}, $\overline{\Delta|Z_i|[i]}$, in the $CaCl_2$–$MnCl_2$–H_2O System

Symbols are the same as in Fig. 7.

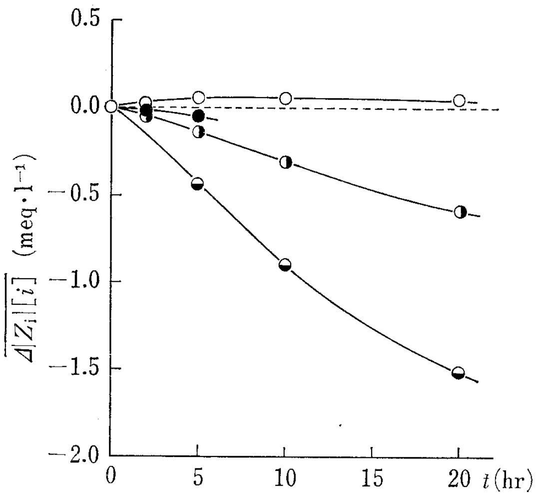

Fig. 11. Mean Concentration Changes of Mn^{2+}, $\overline{\Delta|Z_i|[i]}$, in the NaCl–$MnCl_2$–$H_2O$ System

Symbols are the same as in Fig. 7.

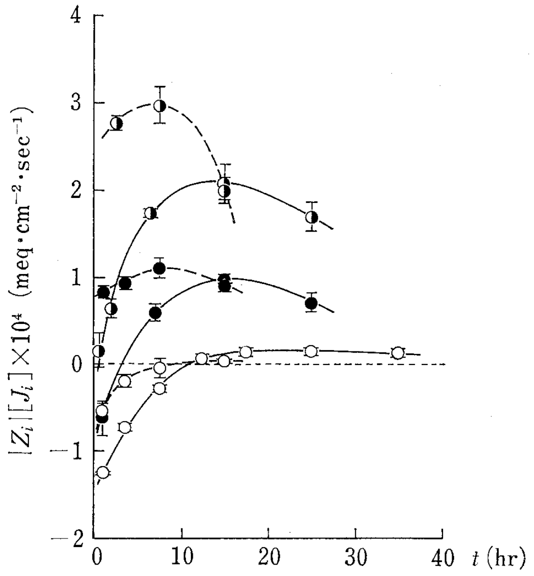

Fig. 12. Flux Changes in the $CaCl_2$–$MnCl_2$–H_2O and NaCl–$MnCl_2$–H_2O Systems

F(Ca/Mn) for Ca system (——) or F(Na/Mn) for Na system (----): 1, (○); 3, (●); 6, (◑).

are two driving forces acting on the ions, *i.e.*, concentration gradient and electric potential gradient. The flux changes in both systems are shown in Fig. 12. The flux can be calculated with the following equation instead of equation (1).

$$|Z_i|[J_i] = \frac{|Z_i|\{V_I([i]_I^{t_2}-[i]_I^{t_1})+V_{II}([i]_{II}^{t_1}-[i]_{II}^{t_2})\}}{2A(t_2-t_1)} \tag{13}$$

V_I and V_{II} are the volumes of the compartments, A is the membrane area, and t_1 and t_2 are times of measurement ($t_1 < t_2$). This is considered to give the value at the mean of times t_1 and t_2.

At the initial stage of permeation, the flux takes negative values in the $CaCl_2$ system when the ratio of concentration of Mn^{2+} in both compartments is 1 or 3, due to reverse permeation. Similarly the flux takes negative values in NaCl system at the initial stage when the ratio of concentration of Mn^{2+} in both compartments is 1. The flux increases gradually and reaches a maximum value in each case. In ordinary membrane permeation, the flux has a relatively large value at the initial stage and decreases with time. When the flux due to the electric potential gradient is opposite in direction and large compared to the flux due to the concentration gradient, the total flux increases with time and reaches a maximum value. If the concentration effect due to such reverse permeation is applicable to biological systems, it should be noted that the outer side of the cell membrane is in contact with a solution in which the concentration of ions does not vary; *i.e.*, since the volume of the outer compartment is greater than that of the inner compartment, the concentration of ions in the outer compartment may be assumed to be constant. Since a static permeation method was applied in this study, the concentrations of ions in comparment I decrease with time. Thus, a larger concentration effect is expected in typical biological systems. It is suggested that Mn^{2+} present in the environment in very low concentrations may be concentrated by reverse permeation due to the effects of other ions coexisting at high concentrations.